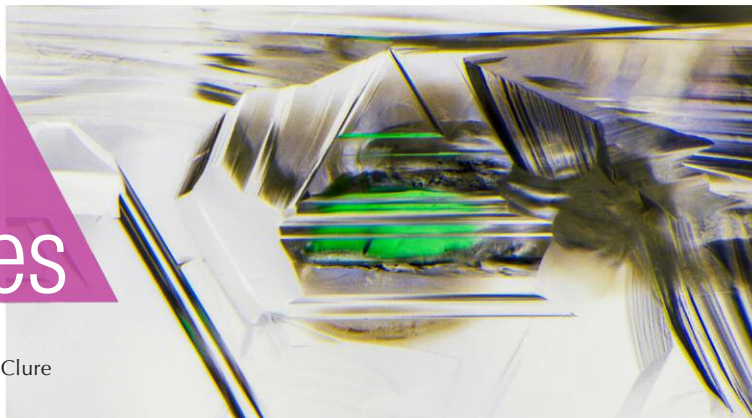


# Lab Notes

## Editors

Thomas M. Moses | Shane F. McClure



## The Largest DIAMOND Ever Discovered in North America

In October 2018, a diamond weighing a remarkable 552.7 ct was recovered from the Diavik mine in Canada. This is by far the largest known gem diamond found to date in North America. It is nearly three times larger than the 187.63 ct Diavik Foxfire which was unearthed from the same mine in August 2015, and about twice the size of a 271 ct white diamond mined from the Victor mine in Canada. GIA's New York laboratory had the opportunity to examine this notable diamond in late January 2019, before it went on public display at Phillips auction house in New York.

This large diamond (54.5 × 34.9 × 31.8 mm) has a striking yellow bodycolor and a rounded irregular ovoid shape (figure 1). The markedly rounded overall shape is due to strong resorption of the crystal surface, leaving a coarse surface texture of complex terraces and hillocks. Negative trigons were sparsely distributed. A fracture oriented perpendicular to the length divides a portion of the diamond, about a quarter of the way in from the smaller end (the left side in figure 1). In and around the fracture there are a few small black inclusions, possibly graphitic or sulfide. At high magnification, a portion of the frac-



Figure 1. This 552.7 ct yellow diamond (54.5 × 34.9 × 31.8 mm) from the Diavik mine in Canada is by far the largest diamond found to date in North America.

ture is slightly resorbed, suggesting that at least part of the fracture developed during ascent in the kimberlite. Patches of surface abrasion up to 7 mm across, but limited to a very shallow depth, are spread widely over the surface. According to a statement by Dominion, these markings are thought to be the result of abrasion during the recovery process, and the fact that the diamond remains unbroken is remarkable.

Infrared absorption spectroscopy reveals that the diamond is type Ia, with a very high concentration of aggregated nitrogen. A very weak absorption at 3107 cm<sup>-1</sup> from the N3VH lattice defect was also recorded. UV-visible absorption spectroscopy reveals strong absorption from N3 (415 nm) and N2 (478 nm), a typical feature of “cape” diamonds. No other ab-

sorption features were detected in the UV-Vis spectrum, consistent with the pure yellow bodycolor visible to the eye. Under long-wave UV radiation, this diamond has strong blue fluorescence and weak but long-lasting yellow phosphorescence. Moderate whitish blue fluorescence and very weak orange phosphorescence were observed under short-wave UV radiation. All these gemological and spectroscopic features are very similar to those observed in the Diavik Foxfire. Photoluminescence analysis at liquid nitrogen temperature with varying laser excitations from the UV to the infrared region revealed additional features of a typical “cape” diamond. Main emission peaks included very strong N3 at 415 nm and weak H3 at 503 nm. In addition, weak emissions at 489, 535, 604, 612, 640, 700, 741,

*Editors' note: All items were written by staff members of GIA laboratories.*

GEMS & GEMOLOGY, Vol. 55, No. 1, pp. 91–101.

© 2019 Gemological Institute of America



Figure 2. This 4.86 ct cabochon displays unusual yellowish chatoyancy against a predominantly purple bodycolor.

787, and 910 nm were recorded. No emission from H4 (496 nm) or H2 (986 nm) was observed.

This diamond has a combination of size, color, and top gem quality that is extremely rare. It will be exciting to see this special diamond crafted into polished form. The Diavik mine is jointly owned by mining companies Rio Tinto and Dominion Diamond Mines.

*Wuyi Wang and Evan M. Smith*

### Chatoyant Quartz/Tourmaline DOUBLET

Doublets are assemblages of two different materials, often joined with cement. Historically they were composed of inexpensive materials used to imitate precious stones. Recently new combinations have been reported, such as a beryl/topaz doublet (Winter 2014 GNI, pp. 306–307), synthetic sapphire/synthetic spinel doublets (Winter 2016 Lab Notes, pp. 418–419), and a beryl/glass complex assemblage (Summer 2018 Lab Notes, pp. 206–208).

GIA's Tokyo laboratory had the chance to examine a unique doublet. The 4.86 ct purplish cabochon, measuring 11.07 × 10.00 × 5.94 mm, appeared to display chatoyancy with a yellowish sheen (figure 2). The hydrostatic specific gravity (SG) and spot refractive index (RI) readings were 2.66 and 1.54, respectively. Assembled fea-



Figure 3. Viewed from the side, the assemblage was obvious. Trapped bubbles in the cemented plane can also be seen.

tures with a cemented plane were easily recognized when viewed from the side, as shown in figure 3. Standard gemological testing, microscopic observation, and infrared spectra revealed that the cabochon segment was a natural amethyst. There were no parallel inclusions that might have caused chatoyancy in this segment. On the other hand, the semitransparent yellowish base had

parallel striations and tube-like inclusions throughout (figure 4). Raman spectroscopy identified the base as tourmaline.

Parallel inclusions located near the bottom of a cabochon can create a chatoyant phenomenon (Winter 2017 Lab Notes, pp. 459–460). This assembled item displayed a similar effect due to the flat tourmaline base with parallel structures. When light was reflected through the amethyst by the tourmaline base, the parallel striations and tube-like inclusions in the tourmaline created the band of reflected light that appeared on the cabochon. Transparent amethyst and semitransparent yellow tourmaline are an uncommon combination. This doublet is an example that assemblages are not always aimed to imitate precious stones but can be creative artworks.

*Yusuke Katsurada*

### Large Faceted GAHNOSPINEL

Gahnospinel is a rare dark greenish blue gemstone that belongs to the spinel group. Its properties result from

Figure 4. Cavities on the base show the parallel striations and columnar or tube-like inclusions. Field of view 1.88 mm.

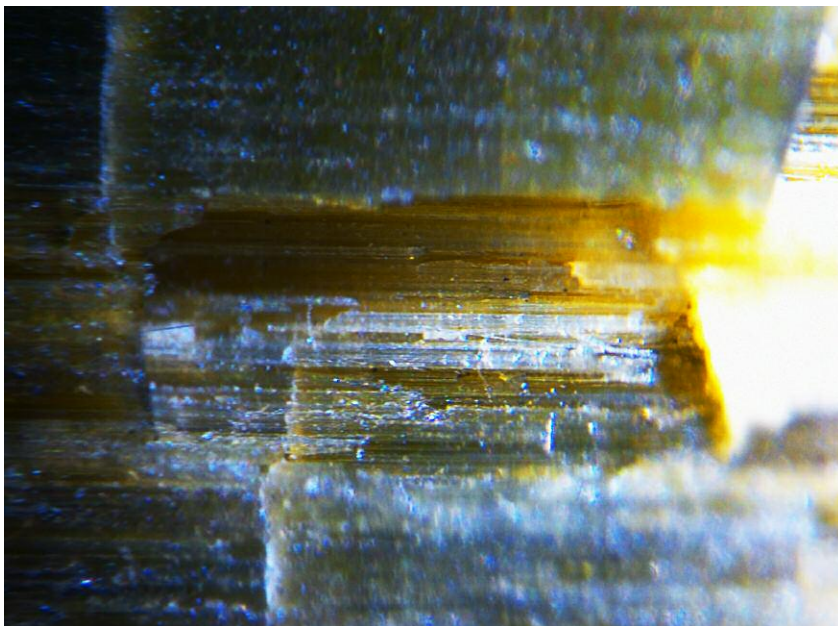




Figure 5. This 11.34 ct gahnospinel was the largest identified by GIA.

being part of a solid solution series with the end members gahnite ( $ZnAl_2O_4$ ) and spinel ( $MgAl_2O_4$ ). Because of the high amount of zinc in the mineral, the RI and SG shift from lower values for the spinel end member to higher values as the amount of Zn substituting for Mg increases, which may lead to confusion when trying to identify it. Spinel has an SG of 3.06 and an RI of 1.718, while gahnite has an SG of 4.55 and an RI of 1.800. As a combination of the two, gahnospinel's SG can fall anywhere in between.

An 11.34 ct transparent faceted oval mixed cut (figure 5) was recently submitted to the Carlsbad lab for an identification report. Despite the

stone's large size, the only inclusions were tiny crystals. To date, this is the largest gahnospinel seen at any GIA laboratory worldwide. The previous stones submitted were 1.95 ct and below.

Standard gemological testing revealed an RI of 1.754 and an SG of 4.10. These results are not typical for spinel. Inductively coupled plasma-mass spectrometry (ICP-MS) data revealed a very high zinc content and the stoichiometry of the sample was calculated to be the following:  $(Mg_{0.485}Zn_{0.385}Fe^{2+}_{0.043})_{0.913}(Al_{2.049}Si_{0.004})_{2.053}O_4$ . The atomic mass of zinc is 65.38, far greater than the 24.31 atomic mass of Mg. As the amount of zinc substitution for Mg in gahnospinel increases, it tends to have a higher RI and specific gravity than spinel. This variety of spinel may bring identification challenges without advanced testing techniques to identify the presence of Zn.

Jessa Rizzo

#### GLASS Bangles

Recently, the Carlsbad laboratory was sent two bangles for identification: a 343.94 ct translucent white bangle and a 355.52 ct translucent mottled light purplish gray and green bangle (figure 6). The white bangle could have easily been given a sight identi-



Figure 7. An elongated gas bubble seen below the surface of the white bangle. Field of view 3.57 mm.

fication of nephrite due to its color and dullness. But its RI of about 1.500 eliminated the possibility of nephrite, which has an RI of 1.62. Further observation showed an even color and no natural inclusions. Gas bubbles of various sizes could be seen just below the surface (figure 7). The RI in combination with the gas bubbles indicated that this bangle was a manufactured product.

The mottled bangle had a color very similar to that of jadeite. An RI of 1.610, rather than the typical jadeite RI of 1.66, indicated that this piece was also not what it appeared to be. Gas bubbles were identified throughout the bangle (figure 8), further confirming that this was a manufactured product. Strings of gas bubbles were observed without mag-

Figure 6. The 343.94 ct translucent white bangle on the left and the 355.52 ct translucent mottled purplish gray and green bangle on the right were carved from manmade glass.



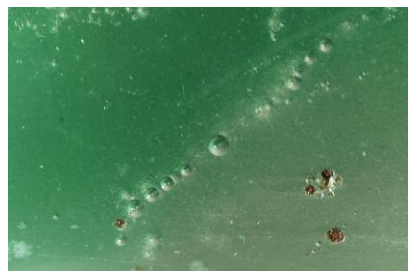


Figure 8. Gas bubbles of various sizes could easily be seen throughout the mottled purplish gray and green bangle. Field of view 3.57 mm.



Figure 9. Clusters of gas bubbles with a string-like structure in the mottled purplish gray and green bangle. Field of view 3.57 mm.



Figure 10. This 1.33 ct brownish orange pear-shaped brilliant cut is the first faceted parisite GIA has examined.

nification, an arrangement that could have easily been mistaken for a natural jadeite structure (figure 9).

These gemological properties and observations identified these bangles as manmade glass and not the nephrite and jadeite they resembled. With nephrite and jadeite having such a rich cultural history, it is common for imitations to show up on the market. Items like these demonstrate the need to always be cautious when purchasing jewelry.

*Nicole Ahline*

### Rare Faceted PARISITE

Recently the Carlsbad laboratory received a 1.33 ct transparent brownish orange pear brilliant for identification service (figure 10). Standard gemological testing revealed a refractive index from 1.670–1.750 with a birefringence of 0.080 and an SG (obtained hydrostatically) of 4.40. There was no fluorescence observed with exposure to long- or short-wave UV light. The stone also appeared doubly refractive when examined with polarized light. Microscopic examination with a fiber-optic light source showed strong doubling, two-phase fingerprints with trapped liquid and gas, and crystal inclusions. Raman and mid-IR spectroscopy conclusively identified the stone as parisite-Ce. The Raman spectrum displayed the strongest vibrational band at 1083  $\text{cm}^{-1}$ , and subsequent peaks at 1740, 1567, 1431,

741, 398, and 269  $\text{cm}^{-1}$ , which positively identified the mineral. The mid-IR spectrum revealed areas of rare earth element (REE) absorption. Energy-dispersive X-ray fluorescence (EDXRF) analysis detected Ce, La, and Ca, supporting this identification.

Parasite is one of the rare-earth carbonite minerals found in the bastnäsite group, with a chemical formula of  $\text{Ca}(\text{Ce,La,Nd})_2(\text{CO}_3)_{3/2}\text{F}_2$ . Parasite crystals are found in carbonatites, granite pegmatites, alkaline syenites, and hydrothermal deposits associated with these environments. Normally the crystals of parisite are too small and cloudy to produce decent gemstones. They are usually found as mineral inclusions in emerald from

the Muzo mine in Colombia and in quartz from Zagi Mountain, Pakistan. This is the first time a faceted parisite gem has been examined by GIA.

*Maxwell Hain*

### Freshwater Bead-Cultured PEARLS with Multiple Features of Interest

GIA's Hong Kong laboratory recently examined a necklace consisting of 24 white baroque-shaped nacreous pearls ranging in size from 21.92 × 15.24 mm

Figure 11. Eleven of the 24 pearls in this necklace exhibited a shape like a dumbbell or peanut shell, which corresponded with the internal twin bead structure revealed by subsequent microradiography.



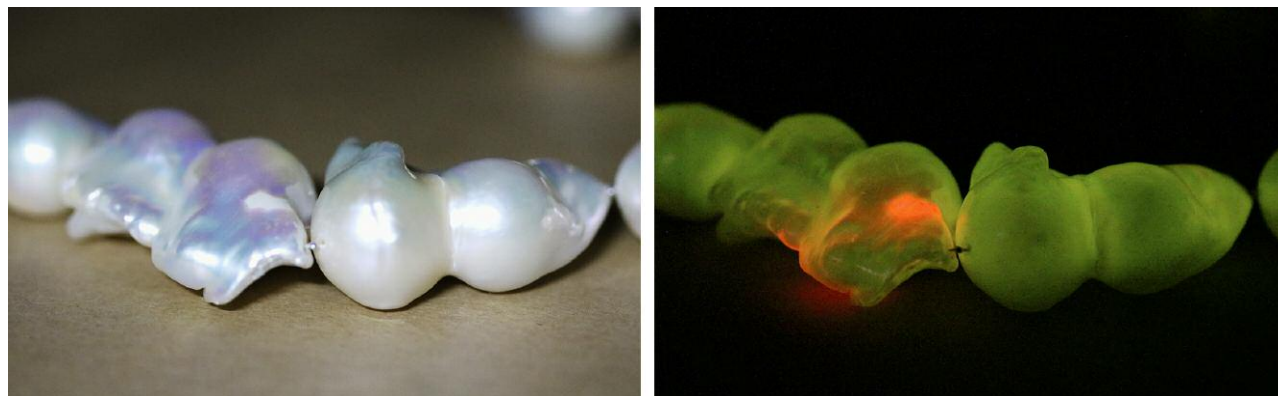


Figure 12. A small whitish non-nacreous region was observed on one pearl under white light (left). The optical X-ray fluorescence image (right) revealed a strong green fluorescence reaction, as expected for freshwater pearls. An atypical reddish orange reaction was observed on the whitish non-nacreous portion.

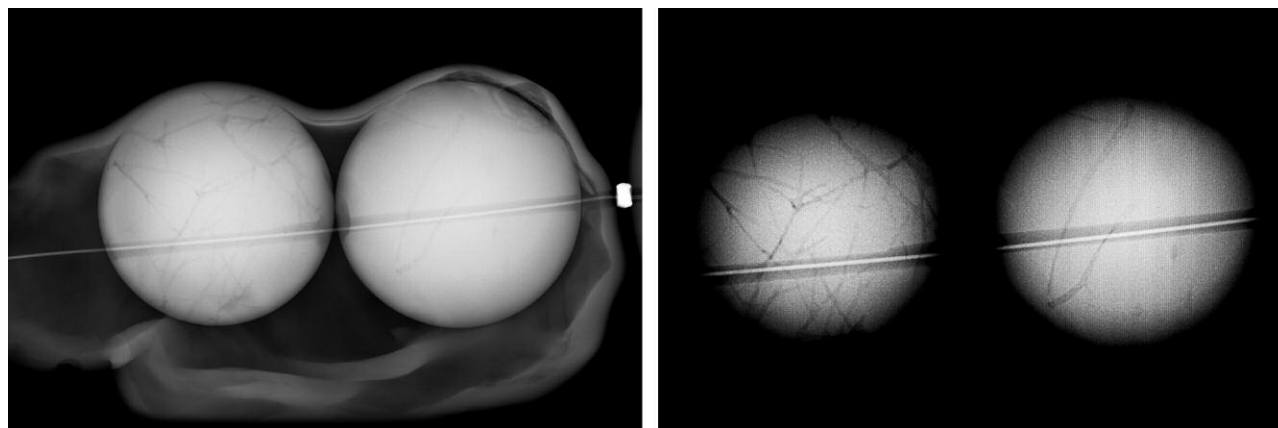
to 24.95 × 15.12 mm (figure 11). Their external appearance, high luster, and strong orient hinted at a freshwater origin. Detailed examination revealed additional features of interest.

While their appearance was indicative of freshwater pearls, energy-dispersive X-ray fluorescence analysis was performed on a random selection to confirm their formation environment. The high manganese concentrations of 751–1728 ppm were consistent with freshwater pearls. In keeping with the reactions seen in freshwater pearls with such levels of Mn, the samples exhibited strong

green fluorescence when exposed to X-rays. However, one in particular displayed moderate to strong reddish orange fluorescence on some areas of its surface (figure 12), associated with whitish non-nacreous regions on the pearl. Similar reddish fluorescence reactions had previously been observed around damaged areas of nacre on pearls examined in GIA's New York laboratory (Summer 2013 Lab Notes, pp. 113–114). The exact reason for this reaction, which GIA gemologists have seen in cultured and natural freshwater pearls from time to time, is unknown.

Eleven of these pearls had a shape resembling a dumbbell or peanut shell, indicating the possible presence of two nuclei in each. Real-time microradiography confirmed the presence of two round bead nuclei in these pearls (figure 13). The remaining 13 contained only a single round bead, consistent with the majority of bead-cultured pearls on the market. In addition, a network of tubules was observed within most of the bead nuclei. Such tubules resembled those observed in saltwater shells, which result from the burrowing actions of parasites. Thus, the bead nuclei were

Figure 13. Microradiographs revealed two round bead nuclei in one of the dumbbell-like pearls (left) and a network of tubules in the beads, resembling the parasite tubes commonly associated with saltwater shells (right). X-ray contrast permits the observation of structures near the surface and nearer the center of the pearls.



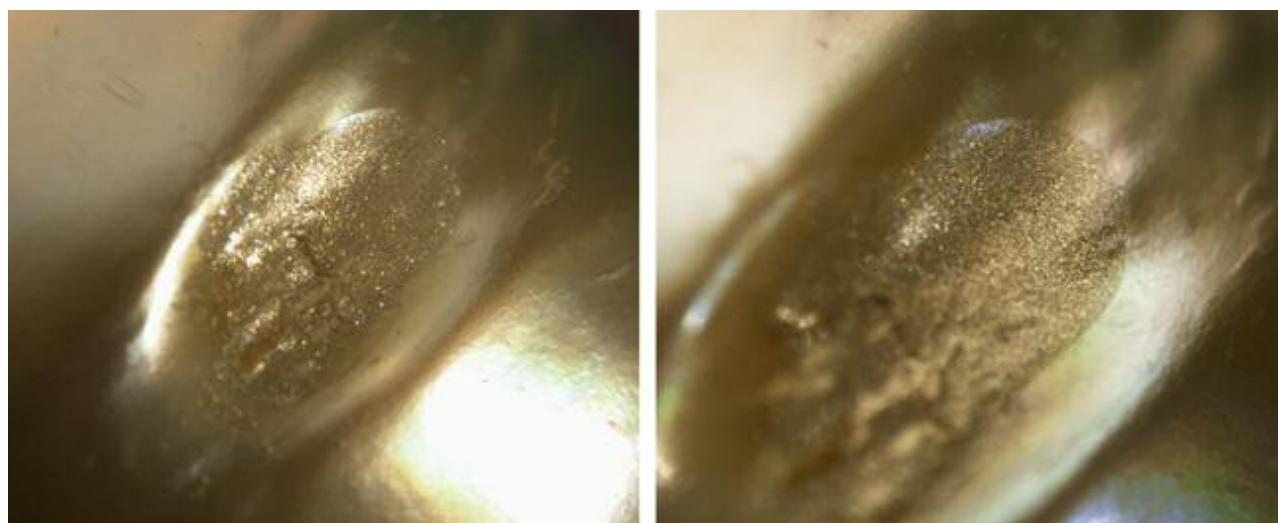


Figure 14. Artificial material was observed filling and masking surface blemishes on some of the pearls in the necklace. Fields of view 5.68 mm (left) and 3.74 mm (right).

likely fashioned from saltwater shells rather than the usual freshwater nuclei employed. Nonetheless, it was impossible to determine the nature of the shell beads without destructive testing. Microradiography examination proved the bead nuclei were not pre-drilled, a characteristic often observed in freshwater nuclei used to culture freshwater pearls (H.A. Hänni, "Ming pearls: A new type of cultured pearl from China," *Journal of the Gemmological Association of Hong Kong*, Vol. 32, 2011, pp. 23–25) and typically encountered by GIA during testing. While pearls cultured with two bead nuclei are relatively uncommon, their existence has been acknowledged in the literature (Fall 1993 Lab Notes, pp. 202–203). The twin bead structure clearly influenced the appearance of these pearls and resulted in some pleasing baroque shapes.

Finally, upon closer examination, a "glittery" grainy material was observed on the pits and blemishes of several pearls (figure 14). This resembled the *essence d'orient* applied on the surface of some imitation pearls. Raman analysis of this material yielded a number of peaks (e.g., 634–639  $\text{cm}^{-1}$  and 1604  $\text{cm}^{-1}$ ) that matched, to some degree, the peaks of the filling material described in an earlier reference (Winter 2017 GNI, pp. 482–484).

While the GIA laboratory examines pearl strands on a daily basis, we seldom encounter one submission possessing several interesting features such as the twin bead structure, reddish orange optical X-ray fluorescence, and filled surface blemishes. It is important for gemologists to always stay alert to the surprises they might find when examining pearls.

Bona Hiu Yan Chow

#### Low-Fe, High-V Color-Change Burmese SAPPHIRE

A color-change sapphire was recently submitted to the GIA lab in Carlsbad

for an origin determination report. The 5.68 ct transparent cushion mixed cut displayed a strong color change from grayish violet in fluorescent light to purple-pink in incandescent light (figure 15). Color-change sapphires generally range from blue to violet in daylight-equivalent (fluorescent) light and from purplish pink to pinkish purple in incandescent light. Stones displaying a strong color-change phenomenon are highly desirable.

Standard gemological testing proved that this stone was corundum with an RI of 1.760 to 1.768. Its weak ruby spectrum displayed absorption lines in the red area between 660 and

Figure 15. This 5.68 ct cushion mixed-cut sapphire showed a strong color change from grayish violet in fluorescent light to purple-pink in incandescent light.



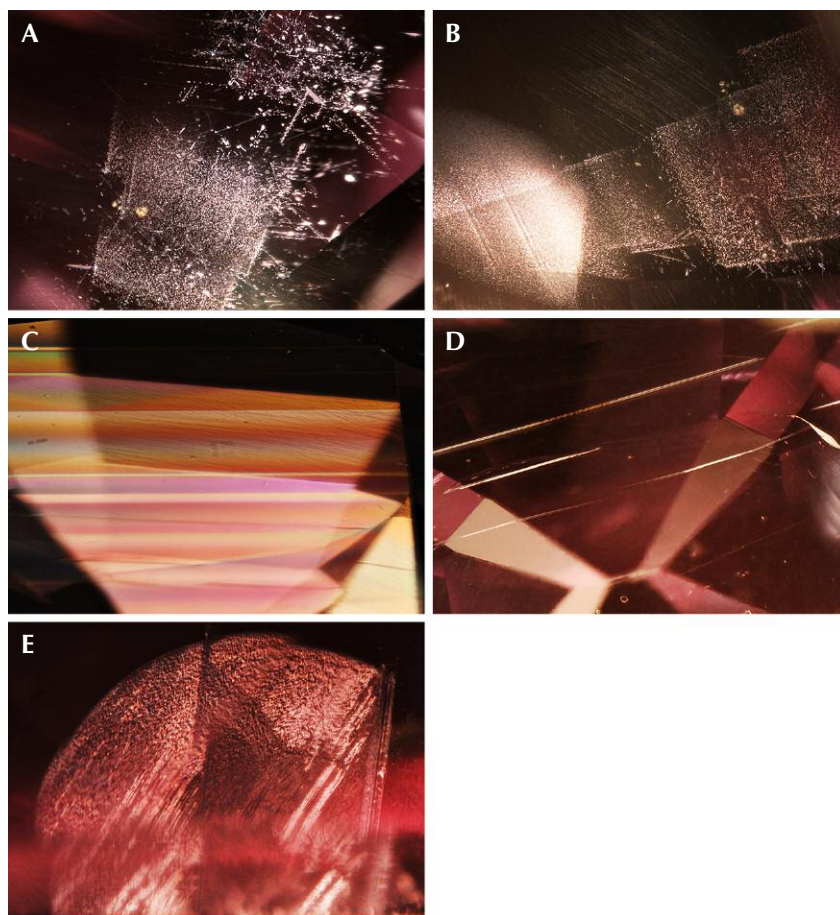


Figure 16. A: Exsolved rutile as reflective platelets, arrowheads, particles, and needles in sapphire; field of view 6.42 mm. B: Loose white particle clouds arranged in a geometric pattern and in stacked planes; field of view 3.80 mm. C: Twinning lamellae are commonly observed in Burmese sapphires; field of view 4.79 mm. D: Boehmite needles or tubules often occur with polysynthetic twinning; field of view 4.79 mm. E: Reflective fingerprints with iridescence in sapphire; field of view 1.37 mm.

695 nm, a broad absorption in the green-yellow area between 500 and 600 nm, and two fine lines in the blue area between 460 and 480 nm. It fluoresced a strong patchy orange color under long-wave UV and a weaker orange under short-wave UV. Microscopic examination revealed exsolved rutile as reflective platelets, arrowheads, particles, and needles (figure 16A); loose white particle clouds arranged in geometric and stacked patterns (figure 16B); a series of twinning lamellae (figure 16C); boehmite needles or tubules (figure 16D); and reflective fingerprints with iridescence (figure 16E). No evidence of heat treatment was observed. The

stone showed diffused pinkish purple zoning in immersion. This inclusion scene is common in but not limited to sapphires from Sri Lanka, Madagascar, and Myanmar (formerly Burma).

To help with the country of origin determination, we collected laser ablation-inductively coupled plasma-mass spectrometry (LA-ICP-MS) chemistry. The results showed very low concentrations of iron, 11–13 ppma, and an unusually high vanadium at 300 ppma.

Several years ago a parcel of color-change sapphires was documented at GIA's laboratory in Bangkok. That material, which had the same unusual chemistry of low Fe and high V,

was from Myanmar. The chemistry profile of our client-submitted stone was consistent with that of the research stones previously documented from Myanmar.

This is the first time the Carlsbad lab has encountered a color-change sapphire with such a unique chemistry profile. LA-ICP-MS again proved to be a useful tool for gemstone origin determination, especially when the inclusion scenes of different localities overlapped.

Rebecca Tsang

### SYNTHETIC DIAMOND CVD Layer Grown on Natural Diamond

A 0.64 ct Fancy grayish greenish blue cushion modified brilliant (figure 17) was recently found to be a composite of synthetically grown and natural diamond. During testing, the infrared spectrum showed both strong absorption of nitrogen and the absorption of uncompensated boron, features characteristic of type Ia and type IIb diamonds, respectively (figure 18). The UV-Vis-NIR spectrum showed “cape” peaks, which are nitrogen-related de-

Figure 17. Face-up image of the natural diamond with CVD synthetic diamond overgrowth. The blue color is due to the boron-doped CVD layer.



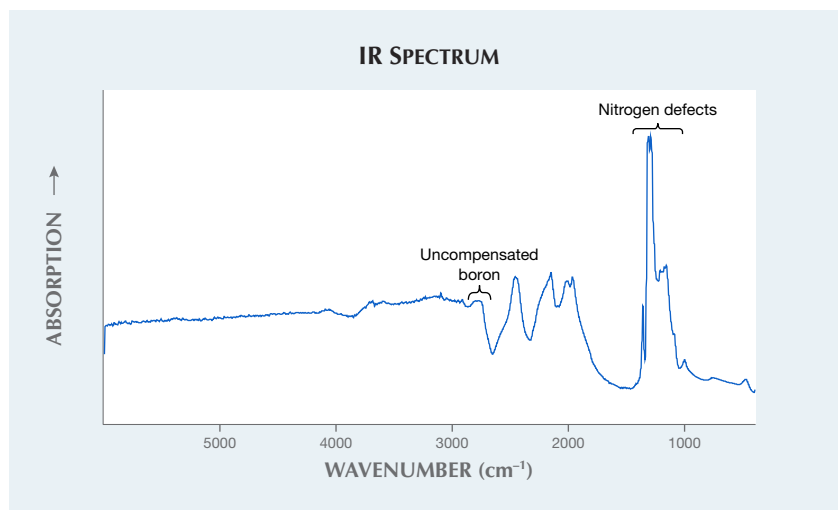


Figure 18. The infrared spectrum shows both nitrogen- and boron-related defects. This combination of defects is very unusual in natural diamonds and a cause for concern.

fects, but also a sloping absorption into the red portion of the spectrum caused by uncompensated boron. It is very unusual for boron- and nitrogen-related defects to be seen together in natural diamonds, though an example has been seen before (Spring 2009 Lab Notes, pp. 55–57). Mixed-type diamonds always call for additional scrutiny.

The DiamondView fluorescence image taken on the pavilion showed a blue hue, caused by luminescence from the N3 defect, and natural growth features. The image taken on the crown showed a greenish blue color common to boron-bearing diamonds and the dislocation patterns characteristic of CVD-grown diamonds. In the image taken from the side, a layer can be seen between the natural substrate and the CVD-grown addition (figure 19). These two distinct fluorescence patterns—the greenish blue from the CVD layer and the darker blue from the naturally grown layer—prove that a layer of CVD synthetic diamond was grown on a natural substrate. A wireframe model generated from a non-contact optical measurement device was uploaded to the DiamCalc diamond modeling program. Using the fluorescence images as a guide, we obtained a 3D section that represented only the

CVD layer. From this, we calculated an approximate layer weight of 0.10 ct and a thickness of approximately 200 microns. A similar diamond previously reported was also a type IIb CVD layer grown on a natural Ia substrate (Summer 2017 Lab Notes, pp. 237–239). That composite was Fancy blue, weighed 0.33 ct, and had a CVD layer that was 80 microns thick.

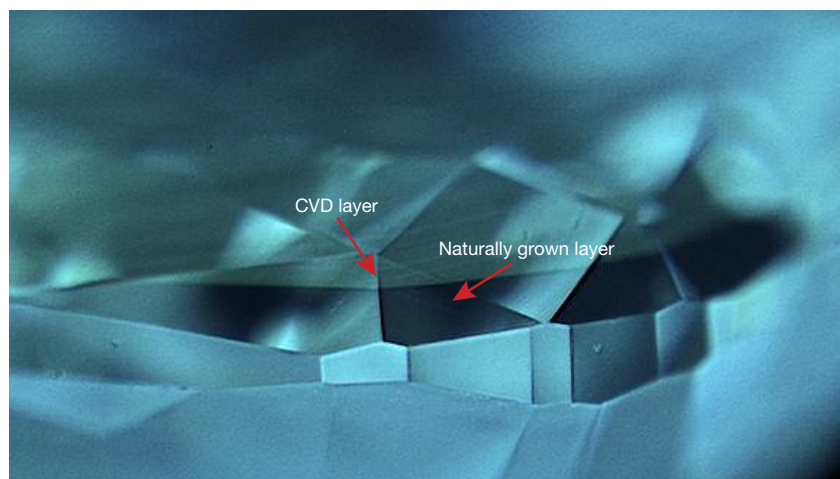
When viewed through a microscope, small pinpoint-like polish features were observed from facet to facet along with a faint line resem-

bling surface graining. These polish features were visible along the entire area of this division and correlated with the separation plane seen in the fluorescence images. Examination with an electrical conductivity tester showed that the crown was conductive but not the pavilion. This is consistent with a type IIb crown and type Ia pavilion.

In immersion, the CVD layer was grayish blue whereas the natural substrate had a yellowish bodycolor (figure 20). The blue color in the CVD layer is from the uncompensated boron, and the yellowish color in the substrate is due to the “cape lines” in the visible spectrum. The final color, Fancy grayish greenish blue, is caused by the gray and blue components from the CVD layer and the yellow from the substrate. The resulting color was likely the main motivation for growing the CVD layer on top of the natural diamond, though the extra weight gained could also be a factor. Viewing under crossed polarizers in immersion revealed dislocation bundles that started at or near the interface and grew upward and outward (figure 21). This proves that it was a thick CVD layer and not a coating of CVD overgrowth.

In CVD-grown diamonds, there is some indication in PL spectra that the diamond has been grown in a labora-

Figure 19. A DiamondView image showing the separation plane.





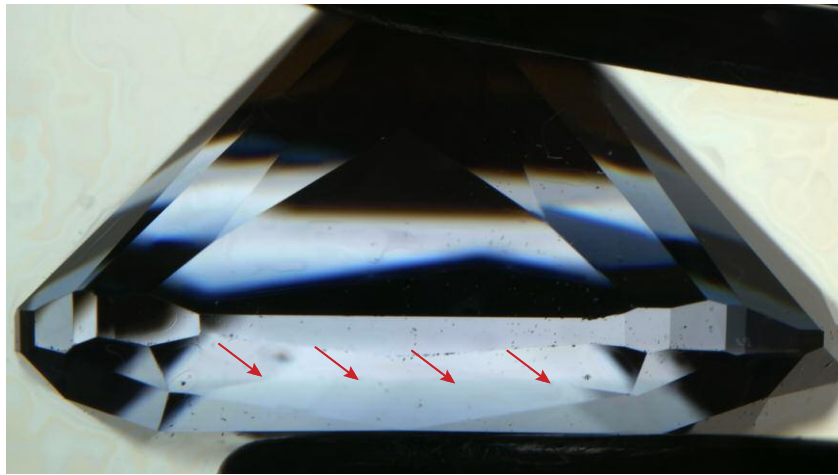


Figure 20. In immersion, the blue color of the CVD layer is clearly visible.

tory—usually the presence of the silicon doublet peak at 736.5 and 736.9 nm or the 596/597 nm defect. Numerous PL spectra were collected in standard and confocal mode on both the crown and pavilion of the diamond in search of any indication of this synthetic overgrowth. In this case, neither of these CVD features were evident, likely due to the thinness of the layer.

With the second of these composites seen at GIA, this could be a new type of product entering the market. Natural diamonds with synthetic diamond grown on the surface require extra scrutiny due to the presence of

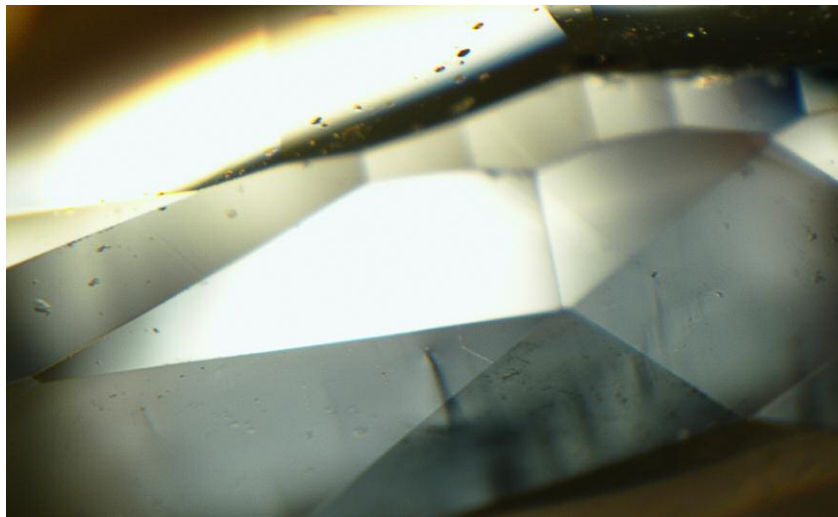
natural-looking features, both spectroscopic and gemological. Careful inspection still reveals the presence of synthetic indicators, which expose the true nature of the diamond.

*Troy Ardon and Garrett McElhenny*

#### Faint Green HPHT Synthetic Diamonds

The Carlsbad lab recently received 25 diamonds for grading reports that all proved to be undisclosed HPHT synthetics, ranging in weight from 0.46 to 0.52 ct. Of these, nine were equiva-

Figure 21. Dislocation bundles in the CVD layer are visible under crossed polarizers in methylene iodide. Field of view 1.90 mm.



lent to the colorless to near-colorless range, eight equivalent to Faint yellow-green, seven equivalent to Faint green (e.g., figure 22), and one equivalent to Very Light green. We found that the green coloration was due to high concentrations of nickel. Nickel is a common impurity in HPHT synthetics, but rarely in amounts significant enough to affect the color.

Previously, GIA gemologists described an HPHT synthetic diamond whose color was equivalent to Fancy Deep yellowish green due to massive amounts of nickel creating an absorption band at ~685 nm (Spring 2017 Lab Notes, pp. 96–98). They showed that the optically active nickel impurities were preferentially incorporated into the {111} growth sectors, as detected by the PL spectral maps and observable color zoning.

Among this set of 25 HPHT synthetic diamonds, none showed the SiV<sup>-</sup> defect at 737 nm with 633 nm PL excitation while 16 showed detectible amounts of uncompensated boron at 2800 cm<sup>-1</sup> in their IR absorption spectra. In this suite, five showed the 685 nm absorption band generally associated with strong nickel impurities while the others showed a broader,

Figure 22. This 0.50 ct HPHT synthetic diamond, color equivalent to Faint Green, owed its color to nickel impurities.



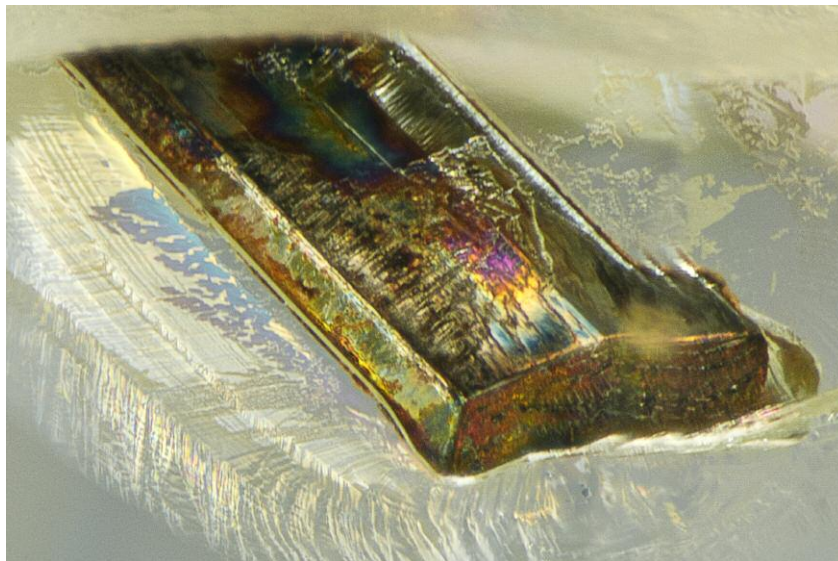


Figure 23. This 0.52 ct Faint yellow-green HPHT synthetic diamond also showed pronounced metal flux inclusions, further proof of its lab-grown origin. This view shows the pavilion facets, with the girdle at the top of the photo. Field of view 1.76 mm.

less pronounced absorption band ranging from 650 to 800 nm. The quantity of uncompensated boron was relatively low, with most containing 0.2–5.6 ppb and one near-colorless sample containing 18 ppb.

Uncompensated boron is also a common impurity in HPHT synthetics, as it is incorporated during the growth process; these low concentrations did not contribute to the coloration. Additionally, several showed distinctive

metal flux inclusions, also indicative of HPHT growth (e.g., figure 23).

Having such a large dataset of similar but unusually colored HPHT synthetic diamonds in the laboratory simultaneously also allowed us to perform additional analyses to compare them. Photoluminescence (PL) maps using 785 nm excitation were collected on the table facet of eight samples, spanning across the various graded colors (figure 24). As expected, the nickel peaks showed the highest concentration within the {111} sectors. From each of the collected maps, we could identify the {111} sectors and determine the average PL intensity of the nickel-related 883/884 nm peaks. When these were plotted according to their equivalent color, the peak intensity was seen to generally increase as the color grade went from the colorless to near-colorless range to Very Light green. Nevertheless, the nickel-related defect at 883/884 nm is not believed to be the same nickel-related defect creating visible absorption. A similar PL map, not shown, was collected on the Fancy Deep–equivalent yellow-green HPHT synthetic diamond (again, see

Figure 24. Left: This PL map, collected with 785 nm excitation, shows that the highest amounts of nickel are concentrated within {111} growth sectors of this 0.52 ct Faint yellow-green HPHT synthetic diamond. This false-color map shows the area of the 883/884 nm doublet normalized with the diamond Raman peak. Right: The average PL intensity of the nickel-related 883/884 nm peak within the {111} sectors increases as the equivalent color increases from colorless to Very Light green.

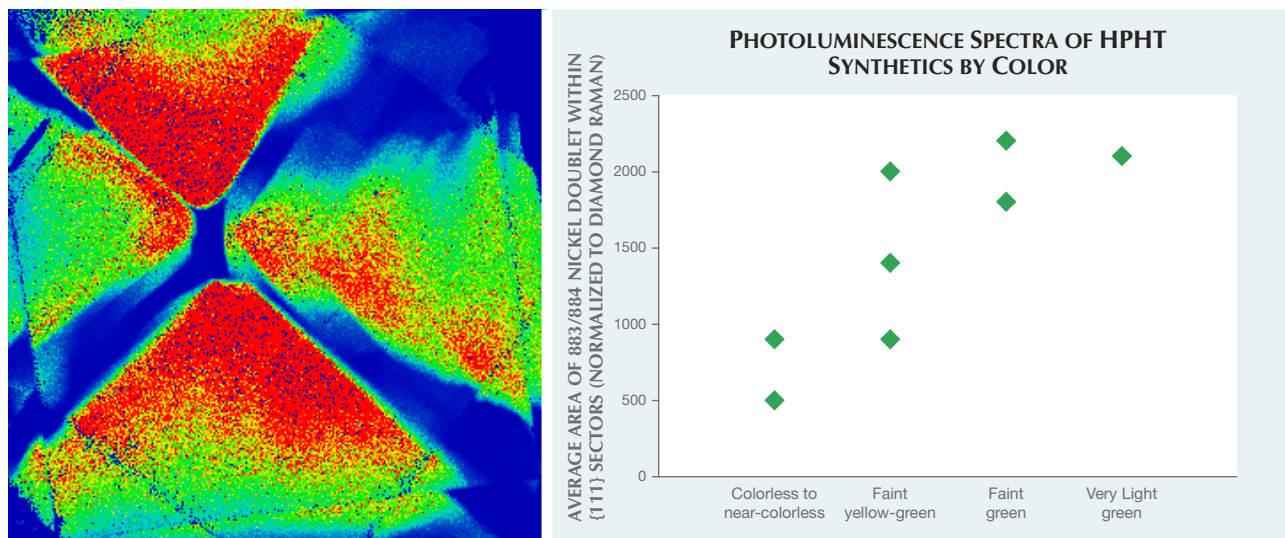




Figure 25. This 7.78 ct round brilliant and 4.90 ct cushion brilliant displayed a blue-green and green-blue color, respectively, that are reminiscent of Paraíba tourmaline.

Spring 2017 Lab Notes, pp. 96–98); the nickel intensity in that case was approximately 10× greater than the Faint green samples studied here.

As laboratory-grown diamond manufacturers continue to experiment with their recipes and the process further evolves, we will likely see greater quantities and a wider variety of color ranges.

Sally Eaton-Magaña

### Paraíba-Like SYNTHETIC SAPPHIRE

Recently GIA's Carlsbad laboratory received for identification two gemstones weighing 7.78 and 4.90 ct (fig-

ure 25) that showed a neon green-blue to blue-green color similar to that of Paraíba tourmaline. Standard gemological testing yielded an RI of 1.76–1.77 and an SG of 4.00, consistent with corundum. Microscopic examination revealed curved color banding (figure 26) when viewed with diffused light and immersed in methylene iodide. Plato lines were observed when examining the stones parallel to the optic axis using cross-polarized light. Curved color banding and Plato lines are the two most important pieces of evidence to separate natural from flame-fusion synthetic sapphire using standard gemological testing. Also observed were wavy, finely textured



Figure 26. Subtly curved color zoning was seen in this vibrant blue-green synthetic sapphire, confirming its flame-fusion origin. Field of view 5.33 mm.

clouds associated with the blue color zones (figure 27). Pink emission caused by the presence of trace-element magnesium was seen only with fiber-optic light. This stone does not react to fluorescent light.

Trace-element chemistry measured by LA-ICP-MS showed the presence of cobalt (105–158 ppmw, with detection limit at 0.652 ppmw), which is presumably responsible for the vibrant color, and magnesium (0.52–1.05 ppmw, with detection limit at 0.044 ppmw). Other trace elements such as Ni, Fe, Cr, and Ti were under the detection limits.

This is the first time GIA's Carlsbad lab has examined flame-fusion synthetic sapphire with a color similar to Paraíba tourmaline.

Forozan Zandi

Figure 27. Blue color zones in the Paraíba-like synthetic sapphires showed wispy clouds when observed with fiber-optic illumination. Field of view 4.95 mm.

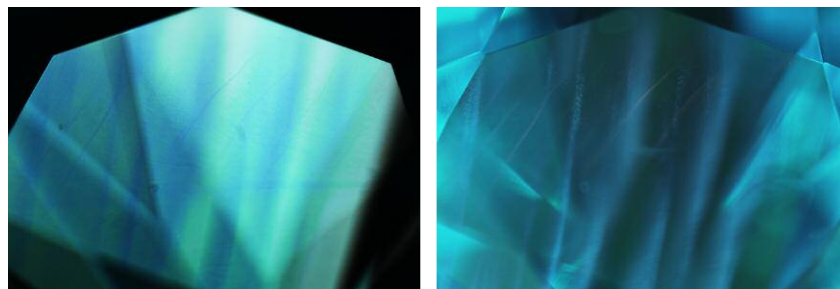


### PHOTO CREDITS

Jian Xin (Jae) Liao—1; Shunsuke Nagai—2, 3; Yusuke Katsurada—4; Diego Sanchez—5; Robison McMurtry—6, 10, 15, 17, 22; Nicole Ahline—7, 8, 9; Johnny Leung—11; Sharon Tsz Huen Wu—12, 13, 14; Jonathan Muiyal—16, 20, 23; Garrett McElhenny—19; Troy Ardon—21; Nathan Renfro—25; Forozan Zandi—26, 27